IMECE2006-13824

ADVANCED PROCESS MODEL FOR POLYMER DERIVED CERAMIC PROCESSING

Xiaolin Wang, Suraj C. Zunjarrao, Hui Zhang, Raman P. Singh
Department of Mechanical Engineering
Stony Brook University
Stony Brook, NY 11794-2300, USA
Email: xiaolinw@ic.sunysb.edu

ABSTRACT

Pyrolysis of preceramic polymers allows a new type of ceramic materials to be processed at a relatively low temperature. The ceramics via polymer pyrolysis display a number of exceptional mechanical, thermal and chemical properties, including high thermal stability, high oxidation/creep resistance, etc. Moreover, they offer better geometrical accuracy compared to conventional ceramics. In addition, thermal induced pyrolysis of organometallic polymer precursors offers the possibility of net shape manufacturing at a lower temperature compared to traditional powder sintering process. The pyrolysis of polymer precursors involves curing of polymer precursors in which the polymer undergoes cross-linking to form a green body, followed by a pyrolysis stage that involves the formation of amorphous SiC and crystallization of SiC at a higher temperature.

The source material changes phase and composition continuously during polymer pyrolysis based ceramic process. Chemical reactions and transport phenomena vary accordingly. To obtain ceramics with high uniformity of microstructure and species without crack, transport phenomena in material processing needs to be better understood and a process model needs to be developed to optimize the fabrication process. In this paper, a numerical model is developed, including heat and mass transfer, polymer pyrolysis, species transport, chemical reactions and crystallization. The model is capable of accurately predicting the polymer pyrolysis and chemical reactions of the source material. Pyrolysis of a sample with certain geometry is simulated. The effects of heating rate, particle size and initial porosity on porosity evolution, mass loss and reaction rate are investigated. Optimal conditions for the manufacturing are also proposed.

NOMENCLATURE

C_p	Specific heat at constant pressure (J/Kg·K)
d_p	Equivalent average particle diameter (m)
E_a	Activation energy (J/mol)
ΔH	Heat of reaction (J/mol)
K	Permeability (m^2)
k	Thermal conductivity (W/m·K)
M	Mass (kg)
$\dot{M}$	Mass change rate (kg/s)
P	Pressure (Pa)
q''	Heat flux (W/m^2)
$\dot{R}$	Reaction rate
R	Universal gas constant, 8.314 (J/mol·K)
r	Radial coordinate
T	Temperature (K)
$T(\phi)$	Tortuosity
t	Time (s)
u	Velocity vector
u_r	Radial velocity (m/s)
V	Volume (m^3)
Y	Species mass fraction
Z	Pre-exponential

GREEK SYMBOLS

ε	Emissivity
ϕ	Porosity
μ	Viscosity (kg/m·s)
ρ	Density (kg/m^3)

SUBSCRIPTS

0	Reference
1	First reaction
2	Second reaction
3	Third reaction

∞	Surrounding
eff	Effective
g	Gas
r	Radial direction
s	Solid
side	Side surface
total	Total

INTRODUCTION

Polymer pyrolysis is a relatively new and very promising technique for processing of advanced ceramics. This processing technique requires much lower energy as compared to sintering route. Moreover, it allows fabricating net-shape components without suffering from maximum components size limitations such as that of chemical vapor deposition (CVD). In addtion, it provides better geometrical accuracy compared to conventional ceramics at much lower temperatures[1, 2]. It also provides flexibility of fabricating refractory ceramic composites.

Novel multicomponent refractory ceramics (carbides, borides and nitrides) have been easily produced by pyrolysis of preceramic precursors in the past decades [3-6]. For example, a number of ceramic products (ceramic foams, bulk composite composites, planar tapes and tubes) have been produced by converting poly (siloxane) resins with methyl, phenyl, vinyl and propyl via pyrolysis route[6]. These ceramics via polymer pyrolysis have shown a lot of exceptional mechanical, thermal and chemical properties, such as thermal stability up to 2000°C, oxidation/creep resistance better than chemical vapor deposition grade polycrystalline nitride and carbide, etc [3-6].

Compared to traditional powder sintering route, thermal induced pyrolysis of organometallic polymer precursors offers the possibility of net shape manufacturing of ceramics at lower temperatures[1]. For example, Si_3N_4/SiC composites are hard to be achieved via conventional sintering of mixture of SiC and Si_3N_4 commercial powders. However, Gozzi *et al* have obtained Si_3N_4/SiC nanocomposite powders from a preceramic polymeric network based on poly(methylsilane) as the *in situ* quasi-stoichiometric SiC source[7]. They have shown potentially high strength, toughness and good creep resistance, and can be used in various high temperature structural applications, such as turbine and automobile engine components and heat exchangers[4-6].

Thermal induced manufacturing of ceramics from polymer precursor systems typically consists of the following steps. The first step is curing of the polymer precursor at 150 °C-250 °C, in which the polymer undergoes cross-linking to form an unmeltable thermoset body. The second step is pyrolysis stage in which amorphous covalent ceramics are formed between 400 °C and 900 °C. The third step is crystallization of ceramics between 1000 °C and 1600 °C [1], in which nanocrystalline materials with microstructures that are stable at very high temperatures are formed.

The source material changes phase and composition continuously during the fabrication. Chemical reactions and transport phenomena vary accordingly. Thus, control of process temperature and reacting species plays an important role in the material property and long-term stability. In addition, transport phenomena in materials processing need to be better understood in order to optimize the process. However, only a limited number of numerical work is available in the literature for polymer pyrolysis. It is important to develop a macroscopic model for predicting the pyrolysis and reaction process in the source material and simulating and guiding the fabrication process. The model should be capable of describing heat transfer, species transport, and chemical reactions of a porous polymer.

In the realm of numerical simulation of polymer pyrolysis, Staggs presented a thermal degradation model for polymers using single-step first-order kinetics[8]. His model is applicable to solve a limited polymer pyrolysis assuming single step reaction. However, polymer pyrolysis is usually more complicated than a simple single-step; the decomposition process may include a number of steps resulting in a set of kinetic equations, one for each step.

In this paper, a model describing the process is formulated via conservation equations of mass, species, momentum and energy for the entire domain. Heat transfer, polymer pyrolysis, chemical reactions, and species transport are combined in the model. Three key reactions for polymer pyrolysis are established. Included in the model formulation are the effects of transport processes such as heat-up, polymer decomposition, and volatiles escape. The model is capable of accurately predicting the polymer pyrolysis of the source material. Pyrolysis of a sample with certain geometry is simulated. The effects of heating rate, particle size and initial porosity on species uniformity and reaction rate are investigated.

EXPERIMENTS AND RESULTS

Allylhydridopolycarbosilane (AHPCS), acquired from Starfire Systems Inc., Malta, New York, USA (SMP-10), is an olefinmodified polymer that undergoes pyrolysis when heated under inert atmosphere and yields near stoichiometric SiC. Carefully weighed quantities of liquid AHPCS were heated, under argon atmosphere, from room temperature up to 300°C, 500°C, 700°C and 900°C, respectively. Samples were held at final temperatures for 30 min to ensure thermal equilibrium. A box furnace was fitted with a retort and modified for inert gas pyrolysis up to 900°C, and pyrolysis beyond 900°C was performed in a specially modified high temperature furnace (Model no. F46248, Barnstead International, Dubuque, Iowa, USA). In addition, small quantities of amorphous SiC derived from AHPCS pyrolyzed at 900°C were heated to different temperatures of 1150°C, 1400°C and 1650°C under a constant flow of argon.

Figure 1 shows the ceramic yield obtained as a function of decomposition temperature. The loss in weight is attributed to the loss of low-molecular weight oligomers and hydrogen gas [9]. About 70–74% ceramic yield in the form of amorphous SiC was obtained in range 900°C–1650°C. The

Copyright © 2006 by ASME

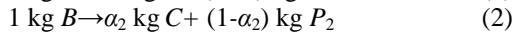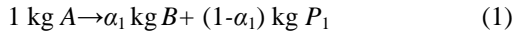material processed to 1150°C is stoichiometric SiC as discussed in [10].

Fourier transform infrared spectroscopy (FTIR) analysis performed on polymer precursor material heated from room temperature to final temperatures of 300°C, 500°C, 700°C, 900°C and 1150°C, respectively, greatly aided the study of polymer to ceramic conversion. Figure 2 shows the IR spectra obtained for products at different temperatures; data is offset to aid comparison. Peaks attributed to C–H (stretching), Si-H (stretching) and Si–C (rocking) bonds were clearly observed in the ranges of 2800–3000cm^{-1}, 2000–2140cm^{-1} and 870–1070cm^{-1}, respectively [9, 11, 12].

These experimental parameters serve as an input to the numerical simulation.

MATHEMATICAL MODEL

Polymer pyrolysis process is characterized with three key steps, as shown in Fig. 3 and Fig. 4. The first step is volatilization (polymer, denoted as A→intermediate product, denoted as B) and occurs in range 300°C –500°C, in which H$_2$ is generated and escaped from the polymer. The second step is crosslink (intermediate product, B→amorphous SiC, denoted as C) and occurs in range 500°C –900°C, in which amorphous SiC is formed. The third step is crystallization of SiC from amorphous SiC (amorphous SiC, C→crystallized SiC, denoted as D) and occurs when temperature is above 1000°C.

These three key reactions are incorporated in the polymer pyrolysis model. The reactions for polymer pyrolysis are expressed as follows:

$$1 \text{ kg } A \rightarrow \alpha_1 \text{ kg } B + (1-\alpha_1) \text{ kg } P_1 \qquad (1)$$
$$1 \text{ kg } B \rightarrow \alpha_2 \text{ kg } C + (1-\alpha_2) \text{ kg } P_2 \qquad (2)$$
$$1 \text{ kg } C \rightarrow 1 \text{ kg } D \qquad (3)$$

where P_1 and P_2 represent volatiles produced from reactions (1) and (2), respectively. It should be noted that reaction (3) is a phase transformation process (amorphous SiC→crystallized SiC).

The following assumptions are made in developing the governing equations:
1. Axial gases flow is neglected since it is much smaller than radial flow
2. The gases flow is transient and laminar
3. The gases and solid phases are at the same temperature locally.
4. Radiation transfer within the polymer can be incorporated into an effective thermal conductivity.
5. The decomposition of the polymer occurs in two steps, according to two first-order Arrhenius processes.
6. The density of polymer remains constant during decomposition.

Figure 5 shows schematic of the model. The crucible is a cylinder, and is 6.22mm in radius and 62.2mm in height. The computational domain consists of gases and solid particles and is considered as porous media. Thus, the porosity of the porous media ϕ is defined as

$$\phi = \frac{V_{total} - V_s}{V_{total}} \qquad (4)$$

where V_s and V_{total} are volume of solid and total volume of the porous media.

Based on the above assumptions and definitions, the conservation of species is given by

$$\frac{\partial [\rho_s (1-\phi)]}{\partial t} = -(1-\alpha_1)\dot{R}_1 - (1-\alpha_2)\dot{R}_2 \qquad (5)$$

where ρ_s is density of solid. Polymer Yield can be obtained based on Eq. (5).

Assuming that the reactions are given by the Arrhenius relation, the reaction rates can be expressed as [13]

$$\dot{R}_1 = (1-\phi)\rho_s Y_A Z_1 \exp(-E_1 / RT) \qquad (6)$$
$$\dot{R}_2 = (1-\phi)\rho_s Y_B Z_2 \exp(-E_2 / RT) \qquad (7)$$
$$\dot{R}_3 = (1-\phi)\rho_s Y_C Z_3 \exp(-E_3 / RT) \qquad (8)$$

where Y_i with i=A, B, C is mass fraction of species i in the mixture. i.e. $Y_i = M_i / M_s$, where M_i, is the mass of species i in the mixture, M_s is the mass of the mixed solid. Z_j with j=1, 2, 3 is the pre-exponential of jth reaction rate, E_j is the activation energy of jth reaction, and R is universal gas constant. The mass change rates of A, B, C, D and the mixed solid are defined by

$$\dot{M}_A = -\dot{R}_1 \qquad (9)$$
$$\dot{M}_B = \alpha_1 \dot{R}_1 - \dot{R}_2 \qquad (10)$$
$$\dot{M}_C = \alpha_2 \dot{R}_2 - \dot{R}_3 \qquad (11)$$
$$\dot{M}_D = \dot{R}_3 \qquad (12)$$
$$\dot{M}_s = -(1-\alpha_1)\dot{R}_1 - (1-\alpha_2)\dot{R}_2 \qquad (13)$$

Two terms on the right hand side of Eq. (13) are mass production rates of volatiles P_1 and P_2 respectively.

The equation of continuity in the cylindrical coordinates is

$$\frac{\partial}{\partial t}\left[\rho_s(1-\phi) + \rho_g \phi\right] + \frac{1}{r}\frac{\partial}{\partial r}\left(\phi \rho_g u_r r\right) = 0 \qquad (14)$$

where r is the radial coordinate, u_r is the radial (convective) gas velocity and ρ_g is density of gas. Axial convection has been dropped due to assumption 1.

The pressure of vapor in the powder can be derived from the Darcy's law:

$$\nabla P = \frac{\mu}{K}u \qquad (15)$$

where K is local permeability of the powder. For a porous media, the expression of K is as follows[14]

$$K(\phi) = \frac{d_p^2 \phi^3}{36 K_0 (1-\phi)^2 (T(\phi))^2} \qquad (16)$$

where d_p and $T(\phi)$ are the equivalent average particle diameter and tortuosity, respectively, $T(\phi)$ is calculated as:

$$T(\phi) = \frac{1}{\phi^{0.4}} \qquad (17)$$

Since we assume only radial velocity, so

Copyright © 2006 by ASME

$$P(r,z) = P_{side}(z) + \int \frac{\mu}{K(r,z)} u_r(r,z) dr \qquad (18)$$

where $P_{side}(z)$ represents vapor pressure at the outer surface of the powder with the axial coordinate z. The fabrication process is related to both temperature and volatiles transport. It is assumed that the volatiles escape from the side surface of the polymer. Therefore, the polymer near the crucible decomposes earlier. The polymer decomposition zone propagates from the side surface of the mixture to the center. The reaction zone size is controlled by porosity and permeability of the porous media.

The heat transfer model determines the temperature distribution that serves as input to the kinetics model. The conservation of energy is expressed as [2, 15, 16]

$$[\phi \rho_g c_{pg} + (1-\phi)\rho_s c_{ps}]\frac{\partial T}{\partial t} + \frac{1}{r}\frac{d}{dr}\left(\rho_g u c_{pg} T\right) =$$
$$\frac{\partial}{\partial x}(k\frac{\partial T}{\partial x}) + \frac{1}{r}\frac{\partial}{\partial r}\left(rk\frac{\partial T}{\partial r}\right) + \sum_{i=1}^{3}\Delta H_i \dot{R}_i \qquad (19)$$

c_{pg} and c_{ps} are specific heat of gases and solid, respectively, k is the effective thermal conductivity of the porous media and ΔH_i i=1, 2, 3 is i^{th} reaction heat.

Since the gas pressure in the quiescent powder is very nearly the ambient pressure, the gas density can be calculated as follows

$$\rho_g = \rho_{g0}(T_0/T) \qquad (20)$$

The internal heat transfer includes both conductive and radiative heat transfer, and for situations in which thermal conductivities of the solid and fluid are not too different. An expression which is a combination of models suggested by Gann *et al* [17] and Kansa[18] is used to model the effective thermal conductivity of a porous media with uniform particles. The expression of k_{eff} is

$$k_{eff} = \phi_{eff}(k_g + \frac{32}{3}\varepsilon\sigma T^3 d) + (1-\phi_{eff})k_s \qquad (21)$$

where ε is emissivity, σ=5.67×10⁻⁸W/m²·K⁴ is Stefan-Boltzmann constant.

RESULTS AND DISCUSSION

The pre-exponentials Z_1 and Z_2 and activation energies E_1 and E_2 are obtained by modeling the pyrolysis of a small polymer sample with lump analysis. Figure 6 shows the comparison of numerical and experimental mass variation (see also Fig. 1) as a function of processing temperature. Z_1 and Z_2 are determined to be 1×10^4 and 2×10^4, respectively. E_1 and E_2 are determined to be 8.3×10^4J/mol and 1.5×10^5J/mol, respectively.

The thermophysical properties used in the simulation are listed in Table 1. Constant heat flux q'' is applied to the boundaries. In addition, we define the polymer yield as the mass ratio between remaining polymer and initial polymer.

The heat flux applied on the boundaries plays an important role in the process. Its effect is studied by comparing the porosity ϕ and polymer yield for three cases

with different heat fluxes: q''=0.3W/m², 0.6W/m² and 1.2W/m². The initial diameter polymer is 100μm. The initial porosity is $\phi = 0.2$, and the reaction time is 20hours. The comparison of temperature profiles is shown in Fig. 7. Figure 8 shows the porosity distribution of three cases. Figure 9 shows the comparison of polymer yield of three cases. The polymer near the crucible decomposes first since the produced volatiles near crucible will escape first. The reaction zone starts from the side surface of the polymer and propagates towards the centerline of the polymer. Its size and propagation are controlled by the porosity and permeability. The temperature increases as heat flux applied is increased. Consequently, the reaction rate increases as shown in Fig. 8.

The effects of particle size d_p on the process are also studied by comparing the porosity ϕ and yield of polymer for three cases with different particle sizes: 20μm, 100μm and 500μm. The initial porosity is $\phi = 0.2$, and the reaction time is 30hours. Figure 10 shows the porosity distribution comparison for the three cases. The comparison of polymer yield is shown in Fig. 11. The reaction zone increases when particle size increases as shown in Fig. 10. Consequently, the reaction rate is increased as shown in Fig. 11. It is because the permeability increases as the particle size increases. The volatiles escape from the porous media becomes faster and the reaction zone and rate increase.

Additionally, the effects of initial porosity on the process are studied. The initial porosities tested are 0.1, 0.2, 0.3 and 0.4, respectively. And the reaction time is 30hours. Figure 12 shows the porosity distribution comparison for the four cases. The comparison of polymer yield is shown in Fig. 13. The reaction zone increases when particle size increases as shown in Fig. 12. Consequently, the reaction rate is increased as shown in Fig. 13. It is because the permeability increases as the porosity increases. The volatiles escape from the porous media becomes easier and the reaction zone and rate increase.

CONCLUSIONS

An advanced process model for polymer pyrolysis based ceramic processing is being proposed. Heat transfer, reactions, species transport and powder porosity evolution are considered in the model. The chemical mechanisms of the process are simplified through apparent kinetic parameters, and the reactions kinetics is established. The effect of heat flux applied to the boundaries on the process is investigated. In addition, the effects of initial porosity and particle size on the processing are investigated. The results indicate that the polymer pyrolysis rate can be increased by increasing the heat flux, increasing the initial porosity, or increasing the particle size.

ACKNOWLEDGEMENTS

Parameter	Value used in program
c_{pg} (J/kg K)	1600
c_{ps} (J/kg K)	1080
k_s (W/m K)	100
k_{gas} (W/m K)	0.1859
ρ_s (kg/m^3)	2500
ρ_g (kg/m^3)	2500
μ (kg/m s)	0.15
E_3/R (K)	2.149×10^{-5}
ε	2×10^4
	0.8

TABLE 1 THERMOPHYSICAL PROPERTIES USED IN THE ANALYSIS AND MODELING
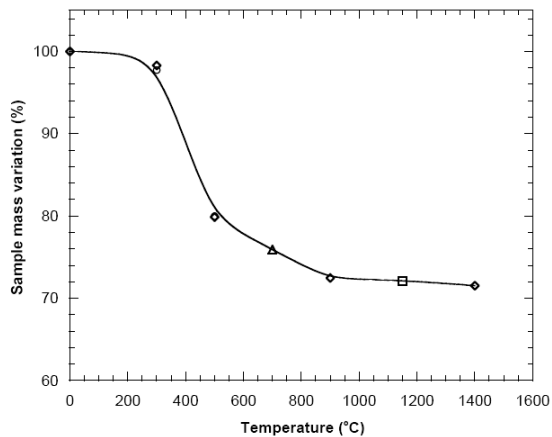
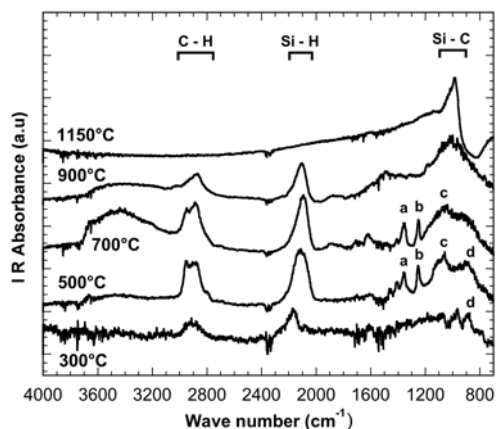FIGURE 1 MASS LOSS VARIATION AS A FUNCTION OF TEMPERATURE FOR AHPCS

FIGURE 2 IR SPECTRA FOR AHPCS HEATED TO 300˚C, 500˚C, 700˚C, 900˚C AND 1150˚C
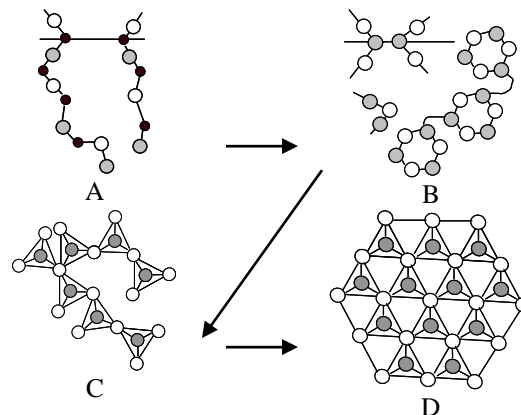
FIGURE 3 SCHEMATIC OF THE POLYMER (AHPCS) PYROLYSIS PROCESS
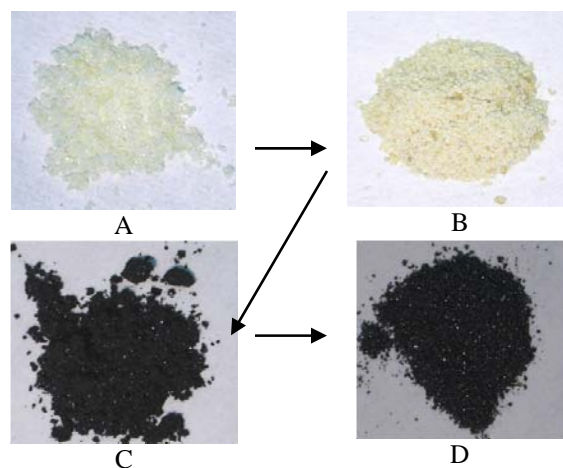
FIGURE 4 IMAGES OF A, B, C AND D
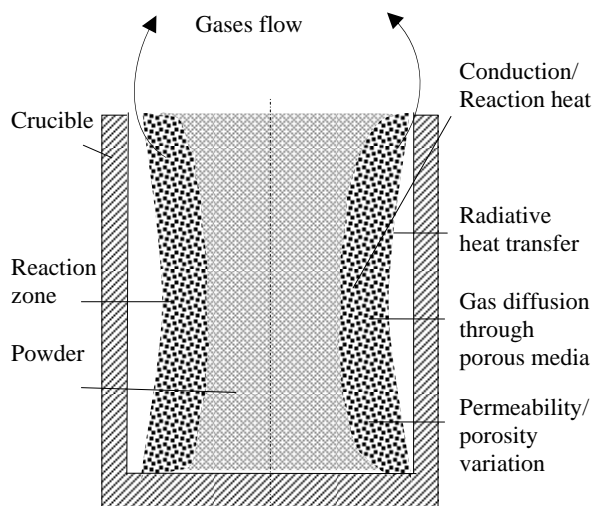
FIGURE 5 SCHEMATIC OF THE COMPUTATIONAL DOMAIN IN THE PROCESS MODEL, THE CRUCIBLE IS A CYLINDER.

5

Copyright © 2006 by ASME
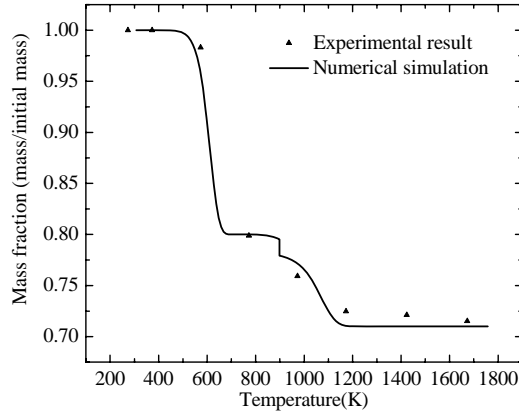
FIGURE 6 COMPARISON OF NUMERICAL AND EXPERIMENTAL MASS VARIATION AS A FUNCTION OF PROCESSING TEMPERATURE FOR AHPCS

(a) q''=0.3W/m^2 (b) q''=0.6W/m^2 (c) q''=1.2W/m^2
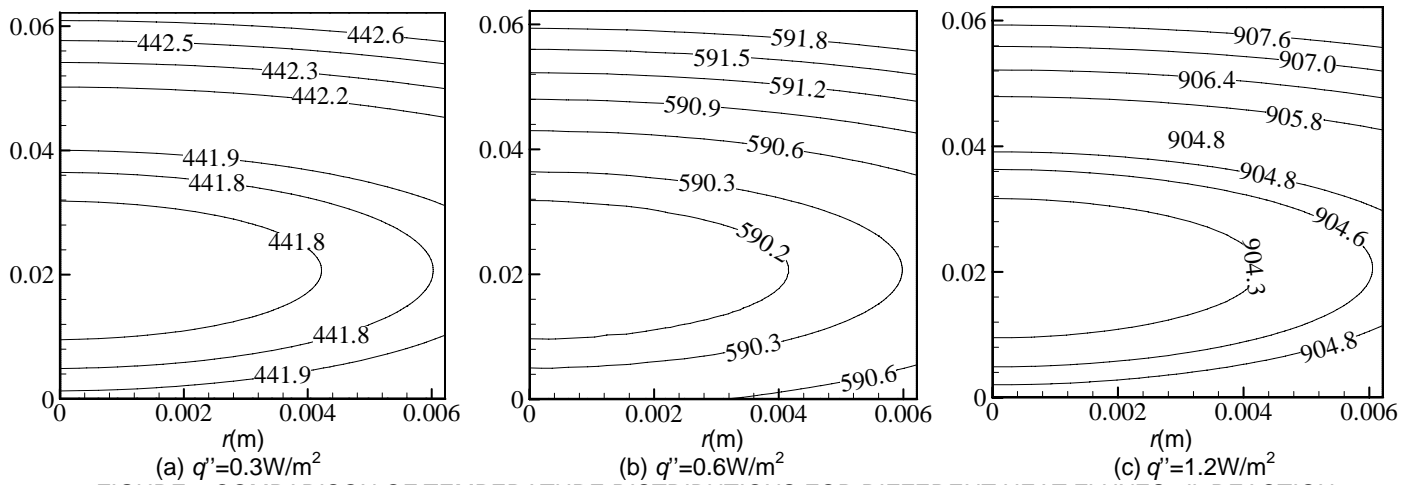
FIGURE 7 COMPARISON OF TEMPERATURE DISTRIBUTIONS FOR DIFFERENT HEAT FLUXES q''. REACTION TIME=20HOURS, INITIAL POROSITY IS $\phi = 0.2$

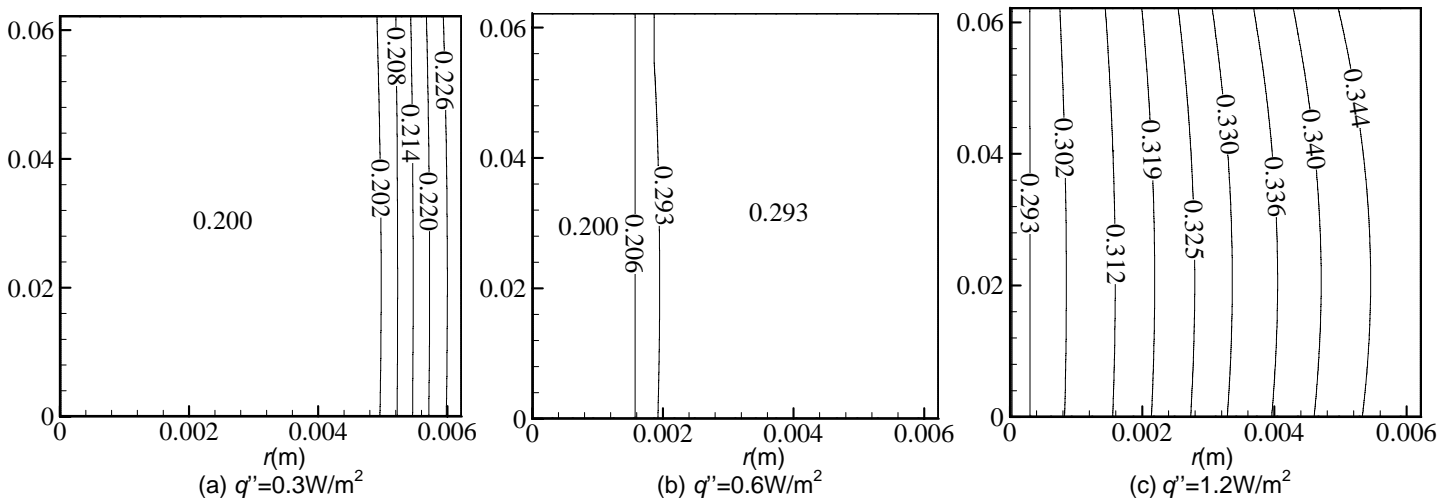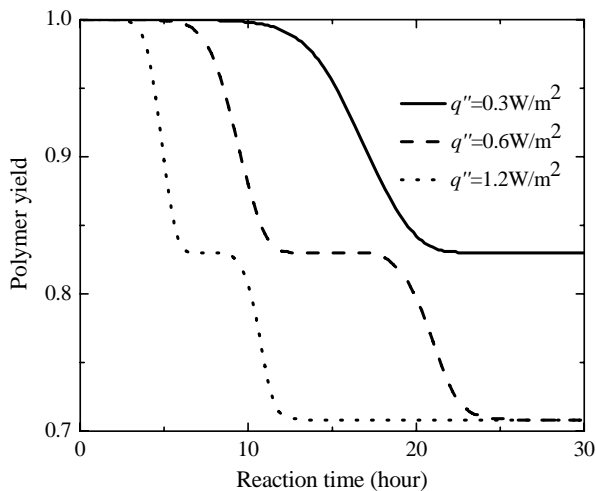(a) q''=0.3W/m^2 (b) q''=0.6W/m^2 (c) q''=1.2W/m^2

FIGURE 8 COMPARISON OF POROSITY DISTRIBUTIONS FOR DIFFERENT HEAT FLUXES q''. REACTION TIME=20HOURS, INITIAL POROSITY IS $\phi = 0.2$

6   Copyright © 2006 by ASME

FIGURE 9 COMPARISON OF POLYMER YIELD FOR DIFFERENT HEAT FLUXES q''. INITIAL POROSITY IS $\phi = 0.2$

(a) d_p=20μm   (b) d_p =100μm   (c) d_p =500μm
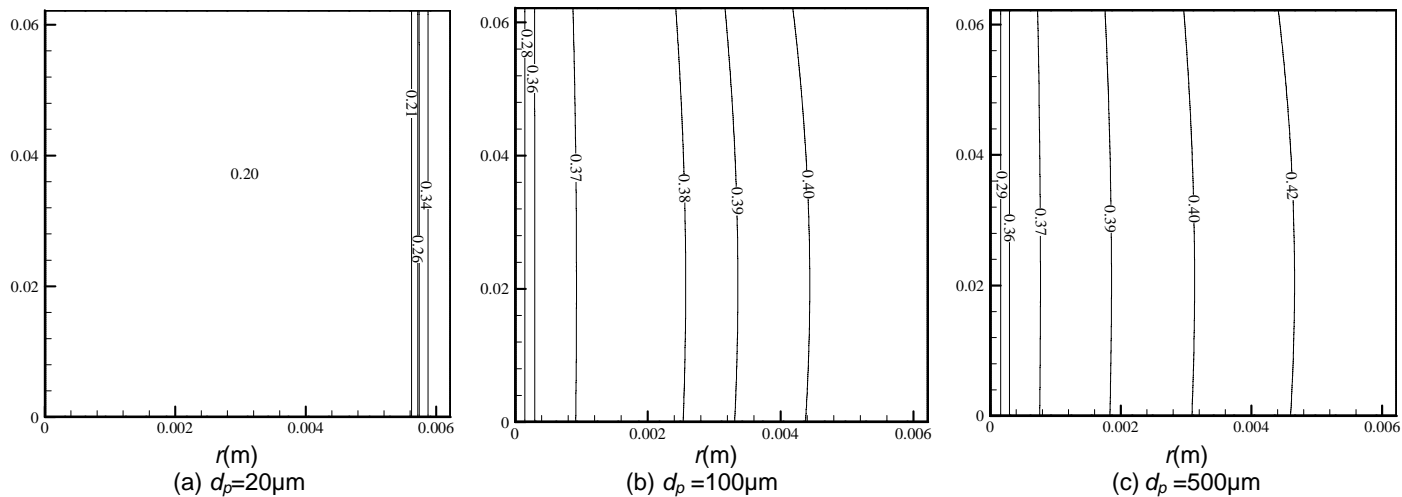
FIGURE 10 COMPARISON OF POROSITY DISTRIBUTIONS FOR DIFFERENT PARTICLE SIZES. REACTION TIME=20HOURS, INITIAL POROSITY IS $\phi = 0.2$
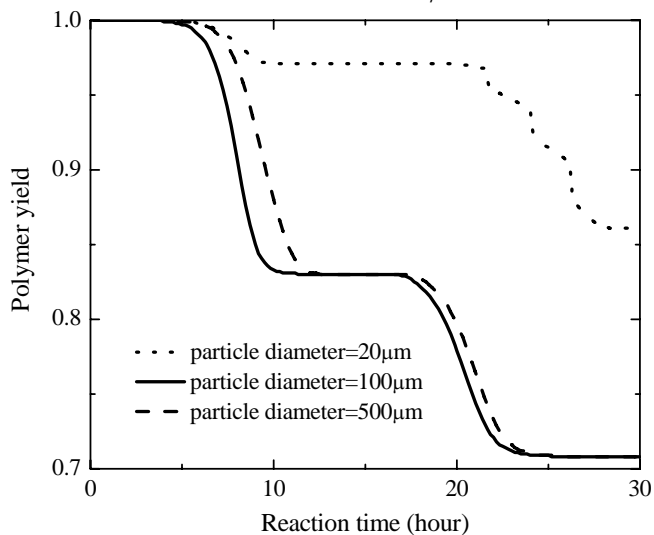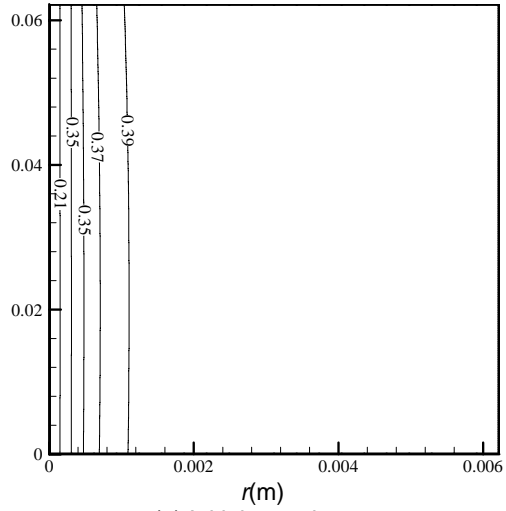

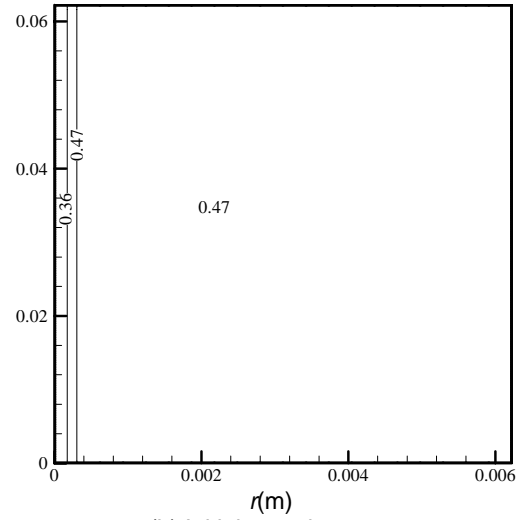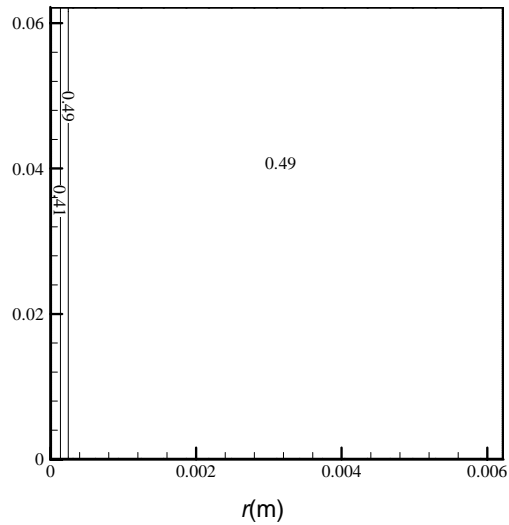FIGURE 11 COMPARISON OF POLYMER YIELD FOR DIFFERENT INITIAL PARTICLE DIAMETERS. INITIAL POROSITY IS $\phi = 0.2$
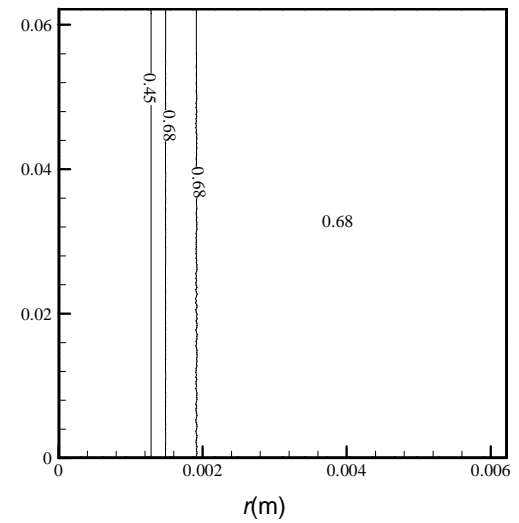
7   Copyright © 2006 by ASME

(a) Initial porosity=0.1

(b) Initial porosity=0.2

(c) Initial porosity=0.3

(d) Initial porosity=0.4

FIGURE 12 COMPARISON OF POROSITY DISTRIBUTIONS FOR DIFFERENT INITIAL POROSITIES. REACTION TIME=20HOURS
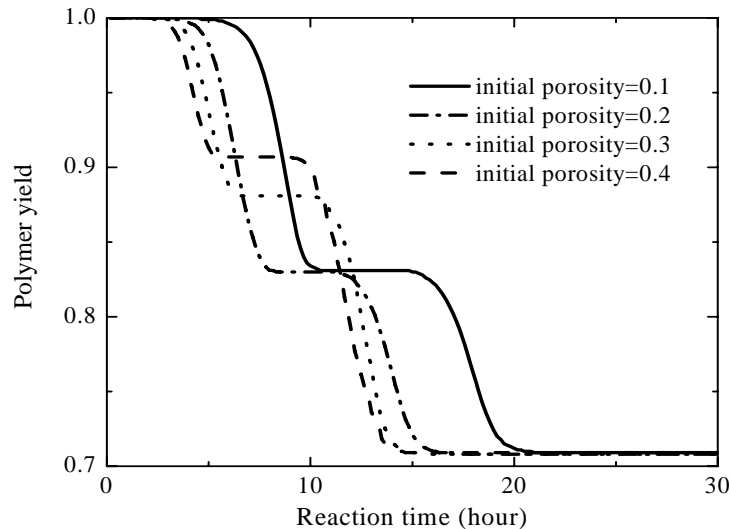
8

FIGURE 13 COMPARISON OF POLYMER YIELD FOR DIFFERENT INITIAL POROSITIES.

REFERENCES

1. Greil, P., *Polymer derived engineering ceramics.* Advanced Engineering Materials, 2000. **6**(2): p. 339-348.

2. Chan, W.C.R., Kelbon, M., Krieger, B., *Modelling and experimental verification of physical and chemical processes during pyrolysis of a large biomass particle.* Fuel, 1985. **64**: p. 1505-1513.

3. Riedel, R., *Advances ceramics from inorganic polymers.* Materials Science and Technology, A Comprehensive Treatment. In Processing of Ceramics, part II, 1996. **17B**: p. 1-50.

4. Kaya, H., *The application of ceramic-matrix composites to the automotive ceramic gas turbine.* Comp. Sci. tech, 1999. **59**: p. 861-872.

5. Sternitze, M., *Review: structural ceramic nanocomposites.* Journal of the European Ceramic Society, 1997. **17**: p. 1061-1082.

6. Herrmann, M., Schuber, C., Rendtel, A., Hubner, H., j. Am. Ceram. Soc. Bull, 1998. **81**: p. 1095-1108.

7. Mauricio F. Gozzi, E.R., I. Valeria P. Yoshida, *Si₃N₄/SiC nanocomposite powder from a preceramic polymeric network based on poly(methylsilane) as the SiC precursor.* Materials Research, 2001. **4**(1): p. 13-17.

8. Staggs, J.E.J., *Modelling thermal degradation of polymers using single-step first-order kinetics.* Fire Safety Journal, 1999. **32**: p. 17-34.

9. Interrante, L.V., et al. *High yield polycarbosilane precursors to stoichiometric SiC. Synthesis, pyrolysis and application* in *MRS Symp.Proc.* 1994.

10. Zunjarrao, S., A. Singh, and R.P. Singh, *Structure-Property Relationships in Polymer Derived Amorphous/Nano-grained Silicon Carbide for Nuclear Applications.* Submitted to 14th International Conference on Nuclear Engineering (ICONE), 2006.

11. Hurwitz, F.I., Kacik, T. A., Bu, X.-Y., Masnovi, J., Heimann, and a.B. P. J., K., *Conversion of polymers of methylandvinylsilane to SiC ceramics.* Journal of Engineering and Applied Science, 1994. **346**: p. 623 – 628.

12. Cullity, B.D., *Elements of X-ray Diffraction.* 1978: Addison-Wesley Publishing Co. Unc., London.

13. Tinney, E.R., *The combustion of wood dowels in heated air.* 10th Symposium (International) on combustion, 1965: p. 925-930.

14. Mota, M., Teixeira, J. A., Bowen, W. R., Yelshin, A., *Binary spherical particle mixed beds: porosity and permeability relationship measurement.* The Filtration Society, 2001. **1**(4): p. 101-106.

15. Sinha, S., Jhalani, A., Ravi, M. R., Ray, A., *Modelling of pyrolysis in wood: a review.*

16. Zhang, H., Moallemi, M.K., Zheng, L.-L. , *Transient Two-Dimensional Numerical Simulation of Laminar Flame Spread Over a porous Fuel.* HTD-Vol. 304, National Heat Transfer Conference-Volume 2, ASME, 1995: p. 53-62.

17. Gann, R.G., Harris, Jr. R. H., Krasny. J. F., Levine, R. S., Mitler, H. E., Ohlemiller. T. J. , *The effect of cigarette characteristics on the ignition of soft furnishings.* 1988.

18. Kansa, E.J., Perlee, H. E., Chailen, R. F., *Mathematical model of wood pyrolysis including internal forced convection.* Combustion and Flame, 1977. **29**: p. 311-324.